Non-linear adsorption characteristics of modified pine wood sawdust optimised for adsorption of Cd(II) from aqueous systems

A. Hashem[a]*, S. M. Badawy[b], S. Farag[a], L. A. Mohamed[c], A.J. Fletcher[d] and G. M. Taha[a]

[a] National Research Center, Textile Research Division, Dokki, Cairo, Egypt.

*Email: (alihashem2000@yahoo.com)

[b] National Center for Clinical and Environmental Toxicology, NECTR, Faculty of Medicine, Cairo University, Egypt.

[c] Microbial Chemistry Department, National Research Center, Dokki, Cairo, Egypt.

[d] Department of Chemical and Process Engineering, University of Strathclyde, 75 Montrose Street, Glasgow, G1 1XJ, UK.

Abstract

The facile modification of pinewood sawdust, with maleic acid, to produce a sorbent aimed at metal ion adsorption, was tested via the batch adsorption of Cd(II) ions from aqueous solution. The sorbent was characterized for the pH of zero point charge (pH_{ZPC}), spectroscopic evaluation of the surface functionalization, structural and morphological features. Factors affecting adsorption behavior, such as adsorbent dose, pH of solution, contact time and Cd(II) ion concentration were investigated. Results obtained show the adsorption rate to be comparatively fast, with equilibrium achieved after ~35 min. Subsequent analysis, showed Langmuirian behavior and a monolayer adsorption capacity of 180.4 mg g^{-1}, at pH 6; while data derived from two-parameter and three-parameter isotherm models was evaluated using non-linear regression methods, with error analysis, to determine the most appropriate model and allow prediction of optimum parameters. The Sips isotherm model proved the most appropriate in describing the experimental data obtained in the study; with a low level of heterogeneity in the adsorption sites occupied suggesting the interaction of the metal ions is

preferential with the added carboxylate moieties only. Additionally, the rate of adsorption was analysed using a range of kinetic models (pseudo-first-order, pseudo-second-order, Bangham and Elovich) in their non-linear forms to provide insight into the adsorption mechanism and showing pseudo-second order behavior is observed, indicating two processes are key in the adsorption process, likely diffusion to the surface and subsequent adsorption on the carboxylate moieties incorporated by chemical modification. In conclusion, the sorbent produced in this study offers high potential for the removal of Cd(II) ions from aqueous solution due to the carboxylic functionalities incorporated into the material, which is optimized by solution pH and adsorbent dose.

Keywords: Maleic acid; Isotherm models; Adsorption kinetics.

1. Introduction

The persistent presence of heavy metals in drinking water, and industrial wastes, has been identified as a global health problem, as these species cannot be biologically degraded like organic contaminants. As a consequence, the removal of heavy metals from water systems has attracted significant attention, which has increased in recent years, with a growing understanding of the toxicity of these species towards human health, aquatic life, flora and fauna[1].

Cadmium has been identified as a major heavy metal pollutant, with a proven high degree of toxicity at very low exposure levels, which can result in acute disorders and various chronic diseases by accumulation in living organisms [2]. This metal is discharged from central industries, like the mining, oil refineries, metal plating, batteries, alloy industries, smelting, phosphate fertilisers and pigments [3-5], resulting in cadmium contaminated water courses.

Adsorption by biomaterials has been proven to be highly effective for the removal of pollutants, including heavy metals from water and wastewater streams, with associated economic benefits, making it a potential alternative treatment route, preferable to conventional techniques such as ion

exchange, precipitation, reverse osmosis and electrode position. Activated carbon is a relatively inexpensive material, which has been used extensively as an adsorbent in wastewater treatment systems but it is unsuitable for developing countries due to the operational cost of such processes[6-8].

Agricultural waste materials offer potential adsorbents in the removal of heavy metals from wastewater [9] and the use of such free resources, which are widely available and incur low processing costs, offers an alternative to the comparatively costly activated carbon, while retaining the favourable physico-chemical properties often associated with latter adsorbents. Sawdust is a natural resource, mainly consisting of cellulose and lignin that has high adsorption capacity for pollutants [10, 11], and has potential for adsorption of key pollutants, such as, heavy metals, oils, dyes and toxic salts from water.

In recent years, modified cellulosic materials has been widely investigated, where potential functional groups are introduced into the material by reaction with hydroxyl moieties present on the backbone of the cellulose chain, which can improve adsorption, or covalent binding, of metal ions [12]. Polysulfide treated sawdust was very effective for the removal of divalent cobalt from aqueous solution [13], while copper-impregnated sawdust exhibits significant arsenic(III) removal [14]. Sawdust treated with phosphates has proven more effective for chromium removal as opposed to untreated sawdust [15]. Dye-treated sawdust was used long time ago for the removal of heavy metal ions from waste water, [16, 17]. The esterification process increases the carboxylic content of the wood fibre surface leading to a corresponding increase in the sorption of divalent metal ions [18]. The cadmium(II) binding capacity of the modified sawdust with carboxyl groups using succinic anhydride could reach uptakes of up to 169 mg g^{-1} [19]. The amidoximated sawdust had a high adsorption capacity for Cu(II) of 246 mg g^{-1} and for Ni(II) of 188 mg g^{-1} [20]. The modified sawdusts using polyacrylic chains possessed 15– 40 times higher adsorption capacity for Cu(II), Ni(II) and Cd(II) than the unmodified sawdusts [21]. The

adsorption isotherms describe the phenomenon governing the mobility of a substance from the aqueous porous media or aquatic environments to a solid-phase at a constant temperature and pH [22, 23].

Based on this rationale, this work is aimed at the modification of sawdust with maleic acid to enhance the adsorption capacity of the resulting material for the removal of Cd(II)ions from aqueous solutions. The effects of altering selected reaction conditions, such as pH, contact time and temperature, on the adsorption capacity of the modified sawdust were investigated, and non-linear regression methods were determine the most appropriate thermodynamic and kinetic adsorption models for this system.

2. Experimental

2.1. Materials and reagents

Pinewood sawdust (SD), obtained from local wood manufacturing companies, was washed with distilled water several times to remove any adhered particles, and subsequently dried at 353 K for 24 h, and sieved to pass through a 50–150 µm mesh. Adsorbent structure and surface moieties were characterised using X-ray diffraction (XRD), Fourier transform infrared (FTIR) spectroscopy, scanning electron microscopy (SEM) and energy-dispersive X-ray fluorescence (EDX) analysis. Cadmium acetate, EDTA, maleic acid, acetic acid, sodium carbonate, acetone and ethyl alcohol were supplied as lab grade chemicals from Merck (Germany), and used as received.

2.2. Methods

2.2.1. Preparation of the adsorbent

The adsorbent was prepared by placing 2 g of SD powder in a beaker and adding a known weight of maleic acid pre-dissolved in water; the resulting mixture was stirred with a spatula. The homogeneous paste obtained was dried in an oven at 373 – 413 K, before subsequent cooling to room temperature. The sample was washed periodically with a solution of ethanol/water (80:20) for 2 h to remove any unreacted maleic acid and soluble by-products, before drying at 333 K for 4 h.

97 **2.2.2. Batch adsorption studies**

98 A weighed quantity of adsorbent (~0.05 g) was added to 100 mL of a Cd(II) ion solution (100–
99 1000 mg L^{-1}) in a 125 mL Erlenmeyer flask. 0.1 M HNO_3 or 0.1 M NaOH was added dropwise to adjust
100 pH values and the mixture shaken at constant speed (150 rpm) at 303 K for a pre-defined period of
101 time, before filtering to separate the metal ion solutions. The concentration of Cd(II) ions was
102 measured before and after adsorption, using direct titration with a standard EDTA solution (0.0005 M).

103 The amount of adsorbed Cd(II) at equilibrium, q_e (mg g^{-1}) was calculated using:

$$q_e = \frac{V(C_o - C_e)}{W} \quad (1)$$

104 While the percentage removal was calculated via:

$$\text{Removal } \% = \frac{(C_o - C_e)}{C_o} \cdot 100 \quad (2)$$

105 where C_o and C_e (mg L^{-1}) are the initial metal concentration and metal concentration at equilibrium,
106 respectively; W (g) is the weight of adsorbent used; and V is the volume of Cd(II) solution (0.1 L).

107 **2.3. Analyses**

108 **2.3.1. Surface chemistry**

109 The pH at zero charge (pH_{pzc}) of the adsorbent sample, also known as the point of zero charge, is the
110 point at which the initial pH value ($pH_{initial}$) equals the final pH of the solution (pH_{final}). This was
111 determined by adjusting the initial pH value ($pH_{initial}$) of 100 ml of 0.01N NaCl solutions in the range 2-
112 12, using 0.01 N HCl solution and 0.01 N NaOH. A 0.1 g of the adsorbent sample was added into each
113 0.01N NaCl solution adjusted to a constant initial pH value. After 24 h, to allow for equilibration, the
114 final pH of the solution (pH_{final}) was recorded and plotted against $pH_{initial}$.

115 FTIR spectroscopy was used to determine the functional moieties present on the surface of the SD
116 adsorbents before and after treatment with maleic acid, and after loading with Cd(II) ions. The

117 averaged FTIR spectra were recorded over 4000–400 cm^{-1} (scan interval: 1 cm^{-1}, number of scans: 120)
118 using KBr discs containing ~2-10 mg of sample in ~300 mg of KBr, on Perkin–Elmer spectrophotometer

119 Carboxyl group contents of the adsorbent samples were estimated [24] by adding 0.2 g of the
120 adsorbent to a 125 mL flask containing 50 mL of NaOH solution (0.03 N). The flasks were left overnight
121 at room temperature, after which their contents were titrated with standard HCl solution (0.01 N)
122 using a phenolphthalein indicator. The carboxyl content of the adsorbent sample was subsequently
123 calculated using:

$$\text{Carboxyl group content} = \frac{100N(V_o - V_i)}{W} = \frac{[COOH]m.eq.}{100\ \text{gsample}} \quad (3)$$

124 where V_o is the volume of HCl (mL) consumed without the addition of the adsorbent in a blank
125 experiment, V_i is the volume of HCl (mL) consumed in the back titration of the adsorbent containing
126 solution, N is the normality of the standard HCl solution (0.XX N), and W is the weight of the adsorbent
127 sample (0.2 g).

128

129 **2.3.2. Adsorbent morphology**

130 The samples studied by SEM were coated with a thin layer of gold using a diode sputter unit, before
131 analysis using a scanning electron microscope (model JEOL-JSM-5600), at an accelerating voltage of
132 25.0 kV. Elemental analysis was performed using an EDX spectrometer (Oxford Instruments 6587 EDX
133 detector), attached to the JEOL-JSM-5600 unit used for SEM.

134 XRD patterns was measured in continuous scanning mode on a PANalytical diffractometer (X'Pert PRO)
135 using a Cu tube. Diffraction intensities were recorded from 2 to 60°, and the diffraction patterns
136 obtained for the samples studied were compared with JCPDS (Joint Committee on Powder Diffraction
137 Standards) patterns.

Textural characterization of materials used in this study was performed using nitrogen adsorption isotherms measured at 77 K, using a Micromeritics ASAP 2420. Isotherms were used to calculate specific surface areas, total pore volumes, *etc*. (see Supporting Information).

2.4. Isotherm Analyses

The experimental isotherm data obtained in this study were analysed using four isotherm models based on two parameters, i.e. Langmuir, Freundlich, Dubinin-Radushkevich and Temkin, and four isotherm models based on three parameters, i.e. Sips, Redlich-Peterson, Khan and Toth.

2.4.1. Two-parameter isotherm models

2.4.1.1. Langmuir isotherm model

The Langmuir Equation [25] is based on monolayer adsorption with a fixed number of localised sites; the model refers to homogeneous adsorption, meaning that the adsorption activation energy and the enthalpies evolved by each adsorbate molecule are equal, in addition there are no interactions between neighbouring adsorbate molecules, nor any site to site movement of adsorbed species. The non-linear form of the Langmuir isotherm is:

$$q_e = \frac{K_L C_e}{1 + bC_e} \qquad 4$$

where C_e is the concentration of Cd (II) ions adsorbed at equilibrium, mg L^{-1}, q_e is the amount of Cd (II) ions adsorbed per unit mass of adsorbent (mg g^{-1}), K_L (L g^{-1}) and b (L mg^{-1}) are constants, and the ratio b/k_L gives the maximum adsorption capacity (q_{max}) in mg g^{-1}. The essential characteristics of Langmuirian behaviour can be expressed in terms of the dimensionless separation factor, R_L, [26] represented by:

$$R_L = \frac{1}{\left(1 + b \cdot C_0\right)} \qquad 5$$

where C_o is the initial adsorptive concentration in solution, and b is a constant. The data presented in

158

159 ***2.4.1.2. Freundlich isotherm model***

160 The Freundlich isotherm can be applied to systems that exhibit multilayer adsorption, mathematically
161 predicting infinite surface coverage at high adsorptive concentrations, and accounts for surface
162 heterogeneity, where the strongest binding sites are occupied first, and the total amount adsorbed is
163 the cumulative adsorption across all surface sites. The decrease in heats of adsorption across all
164 surface sites is assumed to be logarithmic, and the logarithmic form of the model is [27]:

$$q_e = K_F \cdot C_e^{1/n} \quad (6)$$

165 where C_e and q_e are as defined above, and K_F and n are constants related to the adsorption capacity
166 and favourability, respectively.

167 ***2.4.1.3. Temkinisotherm model***

168 The Temkin isotherm model [28] assumes that there is a linear decrease in the distribution of heats of
169 adsorption across all surface sites due to adsorbate/adsorbent interactions, rather than the
170 logarithmic trend assumed in the Freundlich model. The non-linear Temkin isotherm model is
171 represented by:

$$q_e = \frac{RT}{b_T} \cdot ln(A_T C_e) \quad (7)$$

172 where C_e and qe are as defined above, A_T is the Temkin isotherm constant (L g^{-1}), b_T is a constant related
173 to the heat of adsorption (J mol^{-1}), T is absolute temperature (K), and R is the universal gas
174 constant(8.314 J mol^{-1} K^{-1}).

175 ***2.4.1.4. Dubinin–Radushkevich (D–R) isotherm model***

176 The Dubinin–Radushkevich model was developed for adsorption onto a heterogeneous surface where
177 the energy of sites is Gaussian distribution. The non-linear Dubinin–Radushkevich isotherm model is
178 [29]:

$$q_e = q_D \cdot exp\left\{-B_D\left[RT\left(1+\frac{1}{C_e}\right)\right]^2\right\} \quad (8)$$

Where C_e and q_e are as defined above, B_D is a constant related to the free energy of adsorption per mole of adsorbate (mol^2 kJ^{-2}), q_D is a constant related to the degree of adsorption on the adsorbent surface, T is absolute temperature (K). The mean free energy per adsorbate molecule, E (kJ mol^{-1}), can be calculated using:

$$E = \frac{1}{\sqrt{2B_D}} \quad (9)$$

2.4.2. Three-parameter isotherm models

2.4.2.1. Redlich–Peterson isotherm model

The Redlich–Peterson isotherm model [30] combines features from both the Freundlich the Langmuir isotherm models. The non-linear Redlich–Peterson equation is represented by:

$$q_e = \frac{A \cdot C_e}{1 + B \cdot C_e^g} \quad (10)$$

where C_e and q_e are as defined above, A (L g^{-1}) and B are constants, and g is an exponent constant that lies between 1 and 0; when g = 1, Eq. (12) reduces to the Langmuir equation, and when g= 0, Eq. (12) reduces to Henry's equation, where A/(1+B) is the Henry's constant.

2.4.2.2. Toth isotherm model

The Toth isotherm model [31] is another form used to describe heterogeneous adsorption system; it differs by satisfying both low- and high-end concentration boundaries, as expressed by:

$$q_e = \frac{k_T \cdot C_e}{(a_T + C_e)^{\frac{1}{t}}} \quad (11)$$

where C_e and q_e are as defined above, K_T is a constant, a_T is the maximum adsorption capacity, and $^1/_t$ is the Toth exponent constant. It should be noted that this isotherm model reduces to the Langmuir isotherm model, when t is close to unity.

2.4.2.3. Sips isotherm model

The Sips isotherm model [32] is a combined form of the Langmuir and Freundlich isotherm models. The Sips model can be represented by:

$$q_e = \frac{k_s \cdot C_e^{\beta_1}}{1 + a_s \cdot C_e^{\beta_1}} \quad (12)$$

where C_e and q_e are as defined above, k_s (L g^{-1}) and a_s (L mg^{-1}) are constants, and B_s is the Sips model exponent. This model reduces to the Freundlich isotherm model at low adsorptive concentrations, and predicts monolayer adsorption, characteristic of the Langmuir isotherm model, at high adsorptive concentrations.

2.4.2.4. Khan isotherm model

The Khan isotherm model [33] was first proposed to describe the adsorption of aromatics on activated carbons, but is also applicable to the system studied here, and is expressed by:

$$q_e = \frac{q_{max} \cdot b_K \cdot C_e}{\left(1 + b_K \cdot C_e\right)^{a_K}} \quad (13)$$

where C_e and q_e are as defined above, b_k is a constant, a_k is the model exponent, and q_{max} is the maximum adsorption capacity (mg g^{-1}).

2.5. Error analysis

In order to determine the most accurate model of the isothermal data obtained in this study, the error distribution between the experimental data and the data derived from predicted isotherm models

was minimised using error functions. The variance between experimental data and predicted isotherm data (R^2) was optimised using the solver add-in of Microsoft Excel.

The optimization procedure for the isotherm studies requires an error function to be defined to evaluate the fit of the isotherm model to the experimental equilibrium data. The common error functions used here to optimise the isotherm parameters were: average relative error (ARE), average percentage error (APE%), hybrid fractional error function (HYBRID),a determinant of the quality of the fit (χ^2), and normalised standard deviation (Δq%) [34-38] (Table 1).

Table 1: List of non-linear error functions used for data analysis in this study.

Error Function	Equation	References
Average Relative Error (ARE)	$ARE = \sum_{i=1}^{n} \left\| \frac{(q_e)_{\text{exp.}} - (q_e)_{calc.}}{(q_e)_{\text{exp.}}} \right\|$	34
Average Percentage Error (APE %)	$APE\% = \frac{\sum_{i=1}^{N} \left\| [((q_e)_{\text{exp.}} - (q_e)_{calc.}) / q_{\text{exp.}}] \right\|}{N} x100$	35
Hybrid Fraction Error Function (Hybrid)	$Hybrid = \frac{100}{n-p} \sum_{i=1}^{n} [\frac{((q_e)_{\text{exp.}} - (q_e)calc.)^2}{(q_e)_{\text{exp.}}}]_i$	36
Nonlinear chi-square test(χ2)	$\chi^2 = \sum \frac{(q_{e.\text{exp}} - q_{e.theoretical})^2}{q_{e.theoretical}}$	37

Normalized standard deviation $\Delta q(\%)$	$\Delta q(\%) = \sqrt{\frac{Sum[(q_{t.\exp} - q_{t.cal}) / q_{t.\exp})]^2}{(n-1)}} x100$	38

227

228

229 **2.6. Adsorption kinetics**

230 ***2.6.1. Pseudo-first order model***

231 The kinetic process of the pseudo-first order is usually considered physical adsorption and is diffusion

232 controlled. The non-linear mathematical form of the pseudo-first-order model [39] is given by:

$$q_t = q_e[1 - exp(-k_1 t)] \quad (14)$$

233 where q_t is the amount of Cd(II) ions adsorbed (mg g^{-1}) at time t (min), q_e is the amount of Cd(II) ions

234 adsorbed (mg g^{-1}) at equilibrium, and k_1 is the rate constant of adsorption (min^{-1}).

235

236

237 ***2.6.2. Pseudo-second order model***

238 The pseudo-second order kinetic model [46]can be expressed by:

$$q_t = \frac{k_2 q_e^{2\cdot} t}{(1 + k_2 k_e t)} \quad (15)$$

239 where q_t, q_e and t are as defined above, and k_2 (g mg^{-1} min^{-1}) is the rate constant for the kinetic model.

240 This model assumes that the rate of adsorption is controlled by the sharing of electrons between the

241 adsorbent and adsorbate, i.e. a chemical process. The intraparticle diffusion model is not appropriate

242 for studies at high adsorption times. To understand the adsorption mass transfer, the use of

243 approximated models like Weber-Morris (intraparticle diffusion model), is not recommended. Weber-

244 Morris is only valid for short adsorption times and when the bulk concentration is little affect.

2.6.3. Bangham's equation model

Bangham's kinetic model[40] is expressed by:

$$q_t = q_e[1 - exp(-k_b t^n)] \quad (16)$$

where q_t, q_e and t are as defined above, and k_b and n are constants.

3.6. 5. Elovich model

The Elovich kinetic model [41] is expressed by:

$$q_t = \beta ln(\alpha\beta t) \quad (17)$$

where q_t and t are as defined above, α (mg g^{-1} min^{-1}) is the initial rate of adsorption and β (g mg^{-1}) is the desorption constant related to the activation energy of chemisorption, and the extent of surface coverage.

3. Results and discussion

3.1. Characterization of SDTMA

3.1.1. Fourier transform infrared spectroscopy

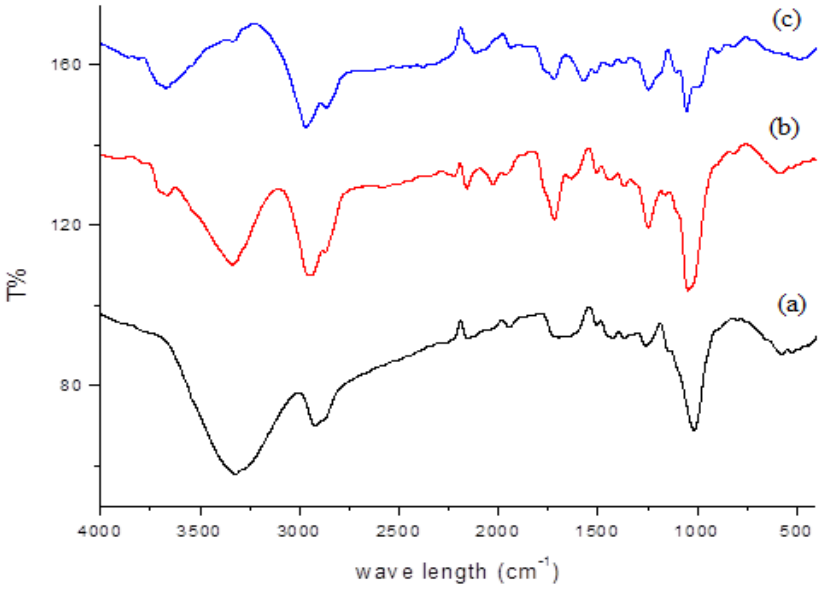

Figure1: FTIR spectra of (a) pinewood sawdust (SD); (b) SD treated with maleic acid (SDTMA); and (c) SDTMA loaded with Cd(II) ions.

The chemical structures of the pinewood sawdust (SD), sawdust treated with maleic acid (SDTMA) and SDTMA loaded with Cd(II) ions, were determined using FTIR spectroscopy (Figure 1). The SD sample (trace a), exhibited a broad absorption peak at 3322 cm^{-1}, indicating the presence of free and bonded O-H, due to vibrations of the hydroxyl groups of cellulose, hemi-cellulose, lignin, and water sorbed on the sawdust. The peak observed at 2923 cm^{-1} corresponds to the stretching vibration of the C-H bond in the methyl groups. The weak peaks at 1695 and 1650 cm^{-1} are characteristic of carbonyl group stretching in ketones and aldehydes, while the strong stretching vibration of C-O (1017 cm^{-1}) is specific to hemicelluloses and lignin components of sawdust [42]. Trace b, in Figure 1, shows the appearance of a strong peak at 1719 cm^{-1} due to the absorption of carbonyl stretching of maleic esters groups. The peak at 1247 cm^{-1} is attributed to the stretching vibration of C-O, associated with carboxyl groups, and the appearance of a weak peak at 1634 cm^{-1}can be attributed to the C=C vibration in the maleate esters. The modification of the sawdust also led to a decrease of the O-H vibration, and an increase of the stretching vibration of the C-O band (1017 cm^{-1}). Trace c shows a decrease in the peaks associated

with of O-H and C-O stretching vibrations, due to complexation with the Cd(II) ions. The appearance of a wide peak at 3671 cm^{-1} is attributed to vibrations of O-H groups from water molecules coordinated to the Cd(II) ions [43].

3.1.2. Scanning electron microscopy

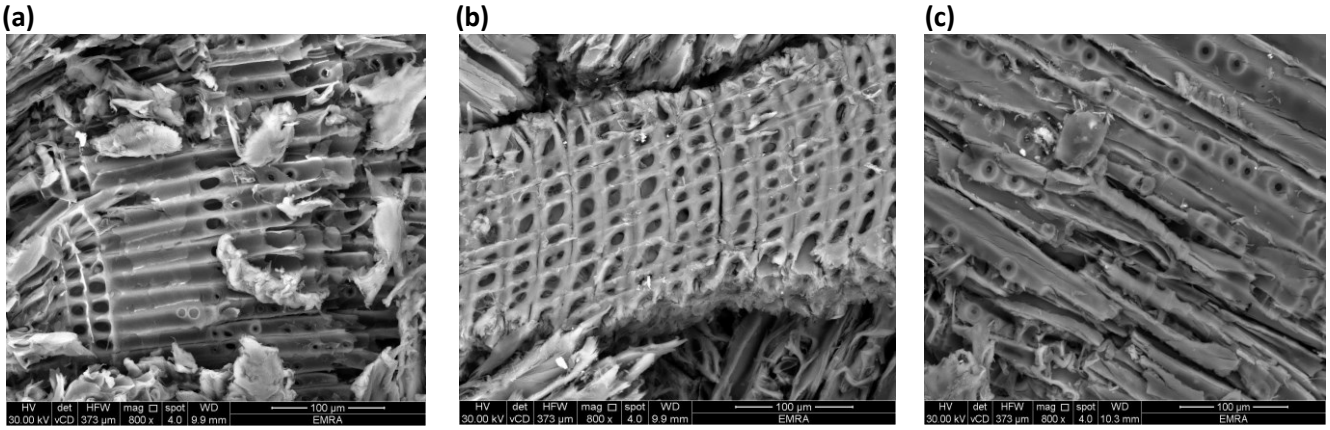

Figure 2: Scanning electron micrographs at 800x magnification of (a) pinewood sawdust; (b) SD treated with maleic acid (SDTMA); and (c) SDTMA loaded with Cd(II) ions.

Figure 2 shows SEM images of SD, SDTMA and SDTMA loaded with Cd(II) ions, at a magnification of 800x. SD appears to be a heterogeneous fibrous structure consisting of rough surface having irregular neat layers shapes with pores and cavities that, in nature, would facilitate the diffusion of an adsorptive and provide a high contact area for adsorption of metal ions (Figure 2a). The fibrous structure, and the fibres themselves, are not intrinsically damaged by maleic acid esterification (Figure 2b). Esterification seems to result in a change in the orientation and length of the fibres to shorter and well-ordered structures. The chemical substitution of cellulose damages some favourable properties of the structure, such as porosity. The average size of the pores, evaluated from the magnified image, was found to be ~5 µm, and these materials present a suitable morphology to retain metal ions. SEM of SDTMA after the adsorption of Cd(II) ions (Figure 2c) seems to show a number of white precipitates on the surface of the fibres, which can be ascribed to adhesion of Cd(II) ions via favourable interactions

295 of the metal ions with ester functional groups of the sample, as supported by EDX analysis, which
296 shows the appearance of Cd signals in the white precipitates (Figure 3).

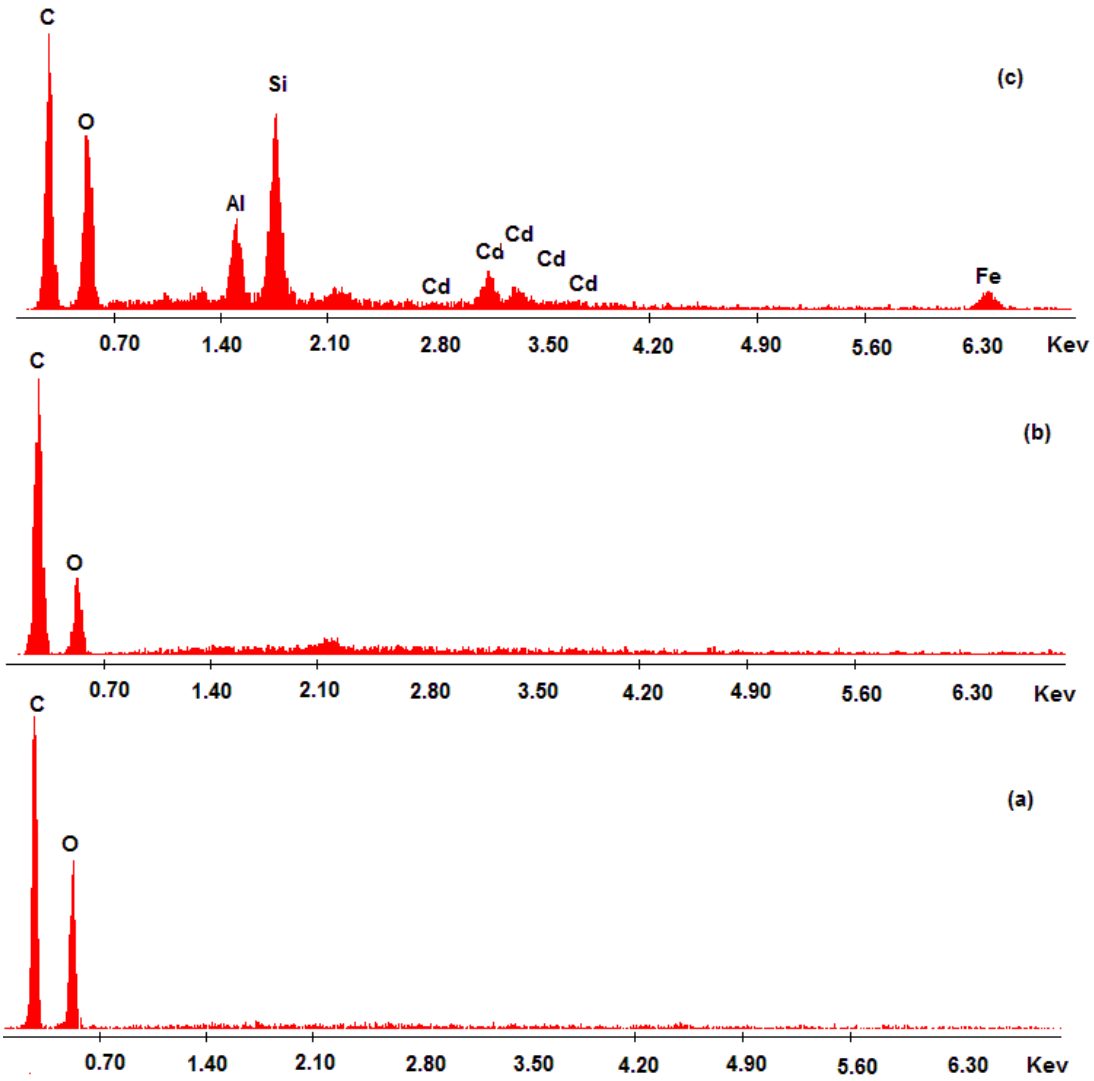

297

298 **Figure 3:** Energy dispersive X-ray spectra of (a) pinewood sawdust (SD), (b) pinewood sawdust treated with
299 maleic acid (SDTMA); and(c) SDTMA loaded with Cd(II) ions.

300

301 **3.1.3. X-ray analysis**

302 XRD uses elastic scattering of X-rays to allow identification of phase purity and the crystalline nature
303 of analysed materials. The XRD pattern of SD (Figure4) shows features typical of a cellulosic material
304 $(C_6H_{10}O_5)_n$, which is the main component structure in wood products, with two broad diffraction peaks,
305 one indicating the crystallinity of cellulose, and a broad amorphous background band. The major peak

306 (100%) at 22.74 degrees (2θ) is an indicator of the presence of highly crystalline cellulose, while the
307 minor one (70%) at 16.66 degrees (2θ) is a measure of the less crystalline content from
308 polysaccharides. XRD after treatment reveals the structural modification of cellulose, as a
309 consequence of esterification with maleic acid, and the appearance of three sharp peaks at 26.54
310 (14%), 38.34 (100%) and 44.59 (86%) 2θ. The characteristic peaks of cellulose do not change in the
311 spectra, indicating that the crystallinity and fibrous structure of the cellulose are not damaged as a
312 consequence of the chemical interaction between cellulose and maleic acid, as indicated above. This
313 indicates that esterification occurs in the amorphous structure of cellulose, not in the crystalline
314 component.

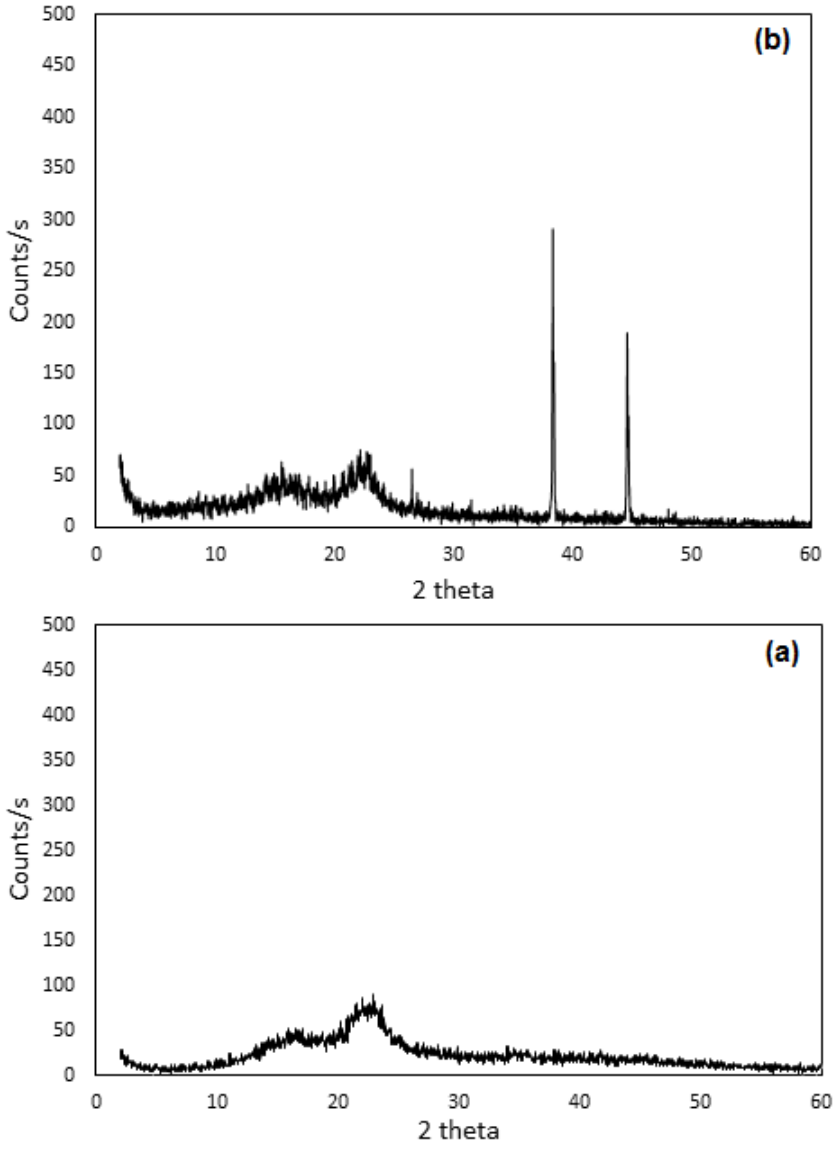

315

316 **Figure 4:**X-ray diffraction spectra of (a) pine wood sawdust (SD) and (b) pinewood sawdust treated with maleic
317 acid SDTMA.

3.2. Modification of SD

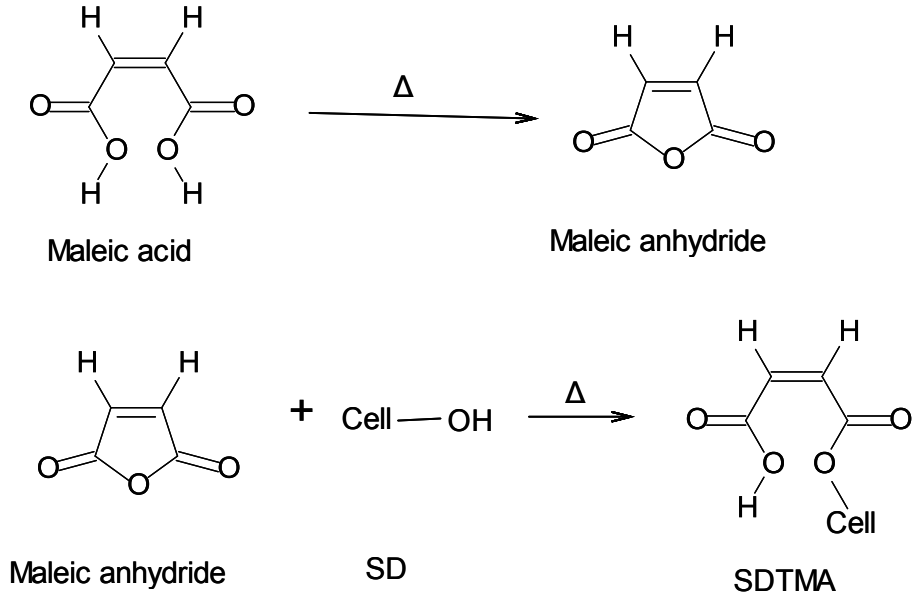

Scheme1: Reaction of pinewood sawdust (SD) with maleic acid (MA) to form pinewood sawdust treated with maleic acid (SDTMA) at high temperature.

In this study, the presence of maleic acid (MA) under a high reaction temperature would allow the formation of maleic anhydride (MAA), which may react with the cellulosic hydroxyls of SD, during such heating, to form sawdust functionalised with maleic acid (SDTMA) as obtained in this study. The proposed reaction pathway is shown in Scheme 1.

The reaction mechanisms for cellulose with maleic acid to form a bond through carboxyl group was described in figure 1.The maleic anhydride may react partially with wood, when a single ester function and a free carboxylic group result, or completely to form di-ester structures [44]. The hydroxyl groups at C-2, C-3 and C-6 of cellulose are reactive and can react with anhydride. The intensity of the peak at 3322 cm^{-1} reduced obviously, indicating that more intermolecular hydrogen bond is destructed compared to the intramolecular hydrogen bond [45, 46].

3.3. Influence of reaction parameters on SDTMA carboxyl content

3.3.1. Effect of maleic acid concentration

Figure 5 shows the effect MA concentration on the extent of functional group incorporation, expressed as m.eq.-COOH 100 g^{-1} SDTMA, for treatment of SD particles with different concentrations of MA. There is, as expected, an increase in carboxyl group concentration, 71.7 to 234.6 m.eq. 100 g^{-1} SDTMAwith increasing MA concentration (4.3 to 69 mmol L^{-1}), the observed trend is an initial sharp increase with an approach to a plateau at higher MA concentration. As the availability of maleic acid molecules in contact with the SD increases, this results in increasing carboxyl content by reaction with the hydroxyl groups present in the parent material, after which carboxyl groups are converted to anhydride groups by dehydration at higher temperatures.

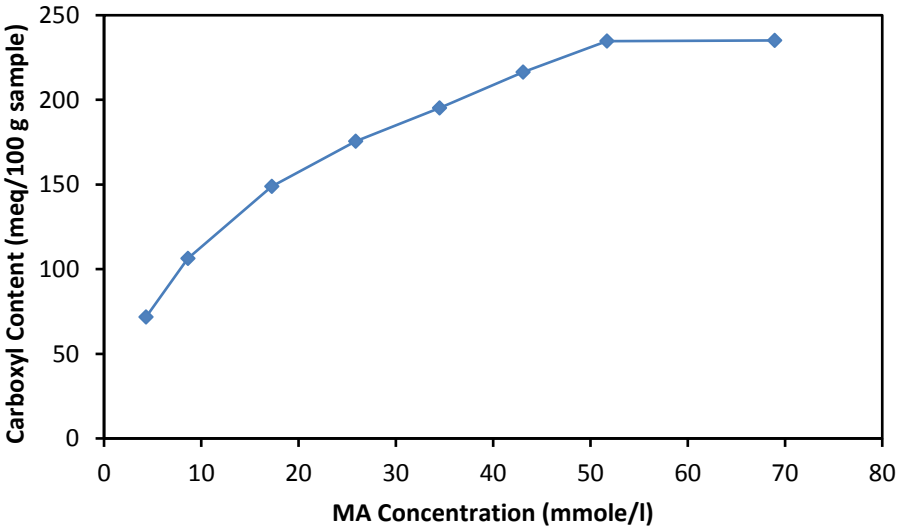

Figure 5: Effect of maleic acid concentration on the extent of modification of pinewood sawdust treated with maleic acid. Reaction conditions: sawdust mass: 2 g; particle size range: 50- 125 µm; reaction temperature: 413 K; reaction time: 1h; carboxyl content: 247 m.eq. 100 g^{-1} sample.

3.3.2. Effect of reaction temperature

Figure 6 presents the results obtained from experiments to study the effect of reaction temperature on the extent of chemical modification of SD particles treated with MA. Carboxyl content increases from 200.8 to 247.2 m.eq. 100 g^{-1}S DTMA as reaction temperature increases from 373 to 403 K;

353 subsequent increase in temperature, above 403 K, results in a decrease in carboxyl content after the
354 maximum is achieved. It is likely that the carboxyl content of SDTMA is enhanced by increasing the
355 reaction temperature to 403 K, as both (1) conversion of MA to MAA and (2) reaction of MAA with
356 cellulosic hydroxyls of SD particles are favoured by higher temperatures. On the other hand, SDTMA
357 is decarboxylated at temperatures higher than 403K.

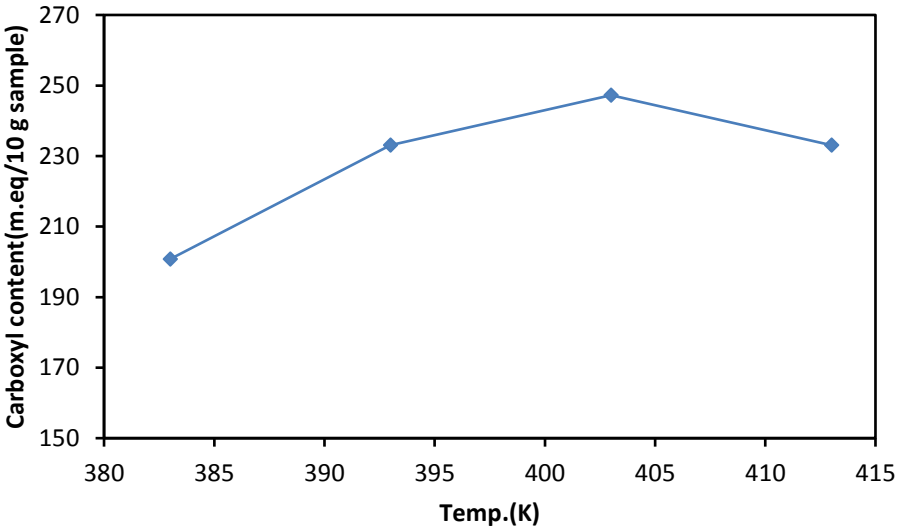

358

359 **Figure 6:** Effect of dehydration temperature on the extent of modification of pinewood sawdust treated with
360 maleic acid. Reaction conditions: sawdust mass: 2 g; particle size range: 50- 125 µm; maleic acid
361 concentration: 51.7 mmol L^{-1}; reaction time: 1h; carboxyl content: 247 m.eq. 100 g^{-1} sample.

362

363 **3.3.3. Effect of reaction time**

364 Figure 7 shows the variation in carboxyl content of SDTMA with changing reaction time. The carboxyl
365 content of SDTMA increases from 225.4 to 242.9 m.eq. 100 g^{-1}SDTMAas reaction time increases from
366 30 to 60 min, before a subsequent decrease is observed at higher reaction times. It is evident that
367 increased time results in increased formation of MAA, which reacts with cellulosic hydroxyl groups to
368 form the carboxyl functionalities observed in the final product of SDTMA. Further time within the
369 reaction system results in catalytic effects on the carboxyl groups and their concentration is decreased,
370 resulting in a final value of 210.71 m.eq. 100 g^{-1}SDTMAobserved at300 min [47].

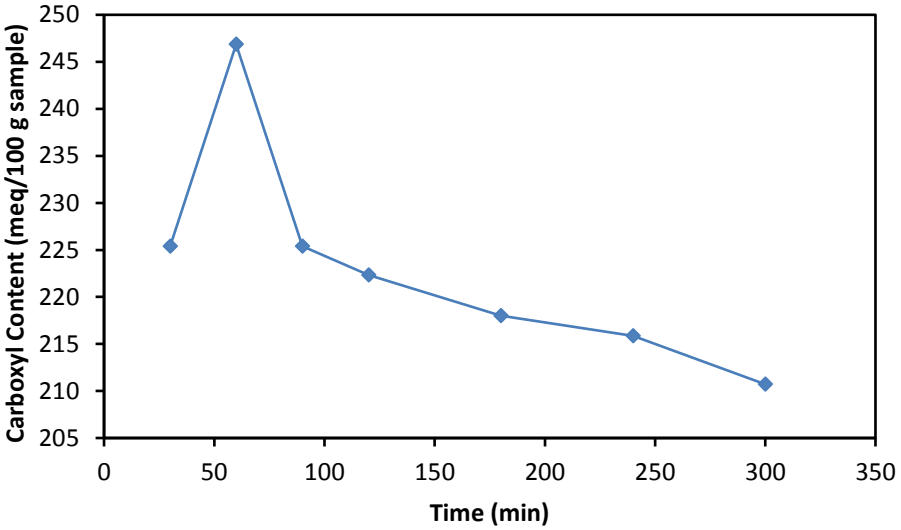

371

372 **Figure 7:** Effect of reaction time on the extent of modification of pinewood sawdust treated with maleic acid.
373 Reaction conditions: sawdust mass: 2 g; particle size range: 50- 125 µm; maleic acid concentration:
374 51.7 mmol L^{-1}; reaction temperature 403 K; carboxyl content: 247 m.eq. 100 g^{-1} sample.

375

376 **3.4. Factors affecting adsorption of Cd(II) onto SDTMA**

377 **3.4.1. Point of zero charge (pH_{pzc}) and effect of pH**

378 The results of studies into the effect of pH on the adsorption of Cd(II) ions by SDTMA, in the range pH
379 3–7, and an initial cadmium ion concentration of 200 mg L^{-1}, are shown in Figure 8.The adsorption of
380 Cd(II) increased from 23 to 136 mg g^{-1} with increasing pH, up to 6, before a plateau is achieved at
381 higher pH. This increase is attributed to ion-exchange processes:

$$2\text{SDTMA-COOH} \leftrightarrow 2\text{SDTMA-COO}^- + 2\text{H}^+ \quad (4)$$

$$2\text{SDTMA-COO}^- + \text{M}^{2+} \leftrightarrow (\text{SDTMA-COO})_2\text{M} \quad (5)$$

382 Deprotonation of SDTMA, the first stage in ion exchange, is shown in Equation 4; the products of which
383 offer adsorption sites for the Cd(II) ions (Equation 5). As can be seen from Figure 8, the adsorption
384 capacity (q_e) of SDTMA towards Cd(II) ions was zero at pH 3, as the presence of a higher concentration
385 of protons causes the equilibrium in Equation 4 to shift to the left, favouring the protonated version
386 of SDTMA and reducing the sites available for Cd(II) ion adsorption. The number of deprotonated sites

387 subsequently increases as the pH becomes less acidic, with a maximum at pH 6. After this point the
388 uptake decreases again, as there is a significant precipitation reaction of cadmium as hydroxide.

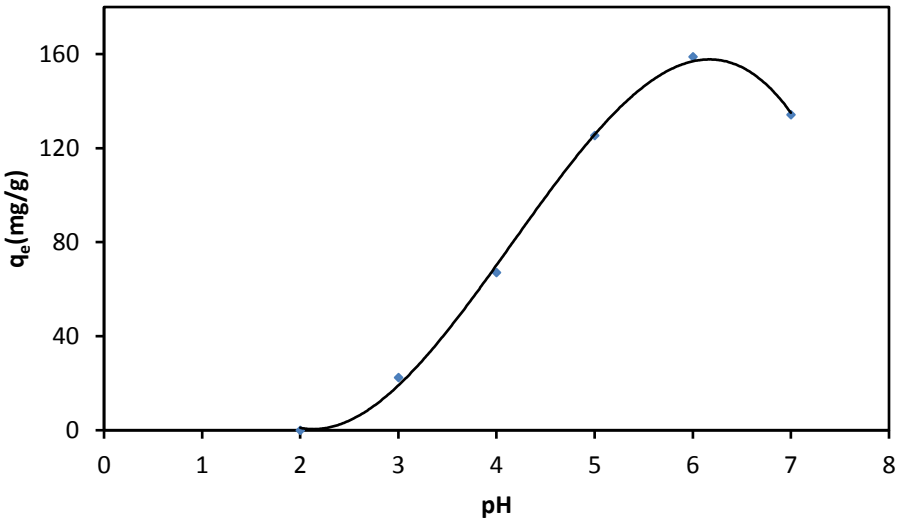

389

390 **Figure 8:** Effect of solution pH on adsorption capacity of pinewood sawdust treated with maleic acid (SDTMA)
391 for Cd(II) ions. Reaction conditions: adsorptive concentration: 300 mg L^{-1}; adsorbent dose: 0.3 g L^{-1};
392 particle size range: 50-125; contact time: 2h; adsorption temperature, 403 K.

393

394 Figure 9 shows the pH_{pzc} data obtained for the surface of SDTMA, which allows the pH at which the
395 surface of SDTMA has neutral charge to be determined. At solution pHs higher than this point of
396 neutrality, the surface will be on the whole negatively charged, likewise, the surface will be positively
397 charged in the main at solution pHs lower than pH_{pzc} [48]. Additionally, pH_{pzc} provides an indication of
398 the electrostatic interactions that occur between the adsorbent surface and the adsorbate [49].The
399 pH_{pzc} of SDTMA was determined as 4, which indicates an acidic nature for the surface of SDTMA. As
400 aforementioned, higher pH values will result in a negative charge on the surface of SDTMA, which
401 favours the binding of cations; conversely, lower pH values will cause a positively charged surface,
402 which makes the adsorption of cations unfavourable [50].

403 As stated in the previous section, the optimum pH for SDTMA to adsorb Cd(II) from solution is 6, which
404 is higher than pH_{pzc}, and leads to a predominantly negative surface charge on the adsorbent surface,
405 resulting in electrostatic attraction with the positively charged Cd(II) cations [51].

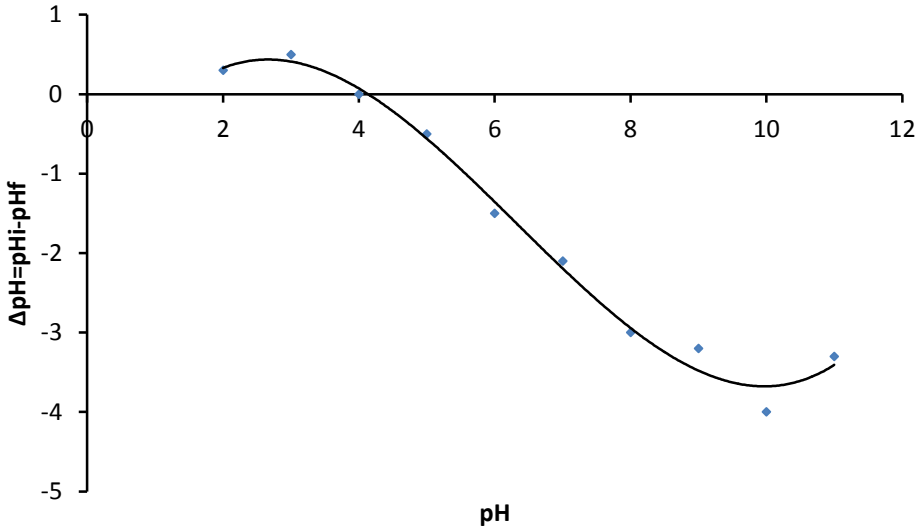

406

407 **Figure 9:** Point of zero charge (PZC) for pinewood sawdust treated with maleic acid (SDTMA).

408

409 **3.4.2. Effect of contact time**

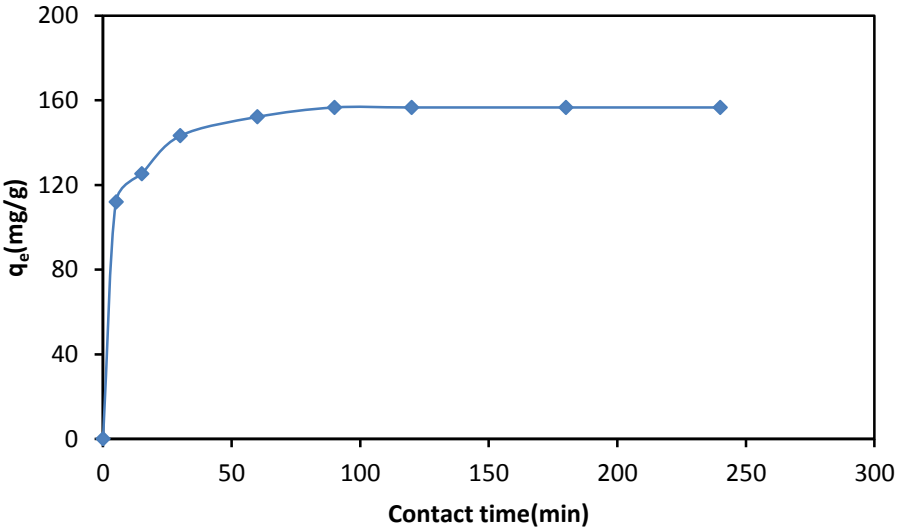

410

411 **Figure 10:** Effect of contact time on adsorption capacity of Cd(II) ions on pinewood sawdust treated with maleic
412 acid (SDTMA). Reaction conditions: adsorptive concentration: 300 mg L^{-1}; adsorbent dose 0.3 g L^{-1};
413 particle size range, 50-125; pH: 6; adsorption temperature, 403 K.

414

415 The effect of adsorption contact time on the capacity of SDTMA towards Cd(II) ions, at an initial
416 adsorptive concentration of 200 mg L^{-1}, is shown in Figure 10. The capacity of SDTMA to adsorb Cd(II)
417 ions increased with increasing contact time, up to an equilibrium at 45 min, after which a plateau is
418 observed and no further improvement is achieved. This equilibrium time is relatively short [52], which
419 is an important consideration in the development of an economically viable wastewater treatment
420 system.

421

422 **3.4.3. Effect of adsorbent dose**

423 It has been previously observed, in many studies, that adsorbent dose influences the uptake of target
424 species from solution, including metal ions. The effect of adsorbent dose on the adsorption capacity
425 of SDTMA for Cd(II) ions was studied at pH 6, using adsorbent doses in the range 0.5–8 g L^{-1}, and an
426 initial metal ion concentration of 200 mg L^{-1} (Figure 11). It can be seen that the adsorption capacity
427 (q_e) of Cd(II) ions, per gram of adsorbent (mg g^{-1}), decreased from 157.1 to 48 mg g^{-1} with increasing
428 adsorbent dose, up to 7 g L^{-1}. With increasing the adsorbent dose, increasing of unsaturated
429 adsorption sites take places, as a result a decrease per unit mass and adsorption capacity of SDTMA
430 for Cd(II) ions decreases, as has been observed previously for Zn(II)[9].

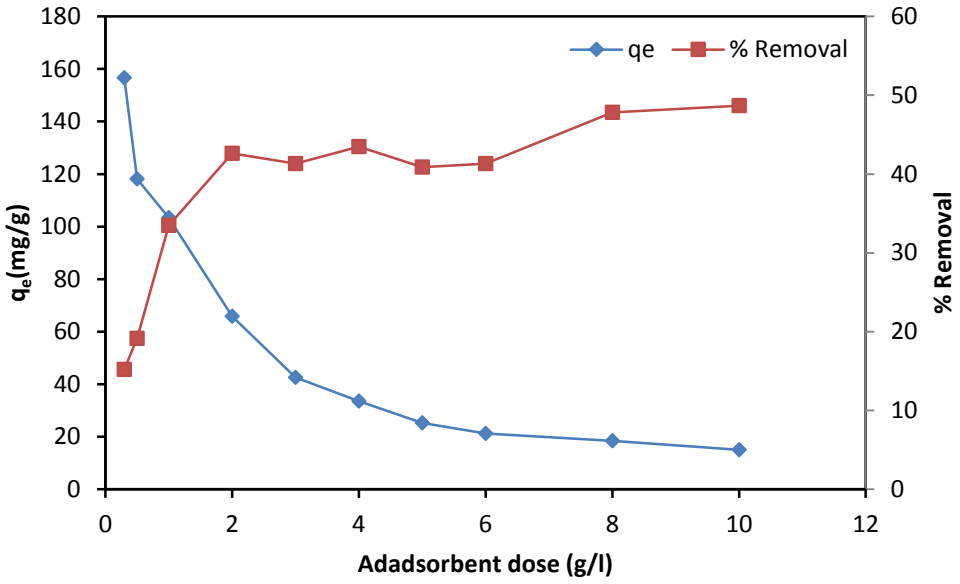

Figure 11: Effect of adsorbent dose (g/l) on adsorption capacity (LHS) and percentage removal (RHS) of Cd(II) ions on pinewood sawdust treated with maleic acid (SDTMA). Reaction conditions: adsorptive concentration: 300 mg L^{-1}; particle size range, 50-125; pH: 6; contact time: 2 h; adsorption temperature, 403 K.

3.5. Isothermal analysis of Cd(II) ion adsorption on SDTMA

An adsorption isotherm describes the thermodynamic equilibrium established between the amount adsorbed on the adsorbent surface with the amount of adsorptive remaining in solution. Several models have been developed to describe the behaviour that may be observed in adsorption systems, and a range of those based on two or three parameters are used to analyse the data obtained in this study, including the two-parameter models of Langmuir, Temkin, Freundlich, and Dubinin-Radushkevich (D-R), and the three-parameter models of Sips, Redlich-Peterson (R-P), Toth and Khan. The isothermal data analysed was obtained for adsorption of Cd(II) ions onto SDTMA, at pH 6, allowing an equilibrium time of 60 min.

The maximum adsorption capacity for Cd(II) ions onto SDTMA, according to the Langmuir isotherm model, was 180.4 mg g^{-1}. Table 2 shows that the SDTMA produced within the present work has a high affinity for the removal of Cd(II) ions (180 mg/g) from solution when compared with

449 wood sawdust raw materials (41 mg/g) and other various adsorbents previously reported in the
450 literature [42, 53-62].

451 Table 2: Comparison of adsorption capacities of various adsorbents for Cd(II)
452

Adsorbent	Adsorption capacity ($mg\ g^{-1}$)	References
Thiol-functionalized magnetic sawdust	4	42
Sawdust grafted with acrylic acid(carboxyl)	168	53
Wood pulpgrafted with acrylic acid(carboxyl)	4	54
Zeolites Clinoptilolite	3.7	55
Zeolites Scolecite	70	56
Organophilic bentoniteClays	2.8	57
Biomass P. chrysosporium	27.8	58
PET was grafted with (2-HPMA)	18.87	59
Coffee grounds waste	15.65	60
Phosphogypsum waste	131.58	61
Wood sawdust	41.21	62
Sawdust treated maleic acid	180.4	Present study

453 Figure 12 shows a comparison between the experimental isothermal data obtained in this study and
454 the theoretical fits offered by the different two- and three-parameter isotherm models described
455 above. Additionally, Tables 3 and 4 present the error analysis and constants for the isotherm models
456 used here. Isotherm type is determined by the value of R_L determined from the Langmuir model data;
457 irreversible when $R_L = 0$, favourable for $0 < R_L < 1$, linear if $R_L = 1$, or unfavourable in the case of $R_L > 1$.

458 The calculated factor of dimensionless separation for Cd(II) ions onto SDTMA is 0.28, while R_L was
459 greater than zero but less than 1, therefore, indicating favourable adsorption.

460 The value of *n* in the Freundlich model (Table 3) was 4.18, satisfying $0 < n < 10$, which also
461 indicates that adsorption of Cd(II) ions onto SDTMA is favourable. The value of $^1/_n < 1$ suggests a slight
462 suppression of adsorption at lower equilibrium concentrations.

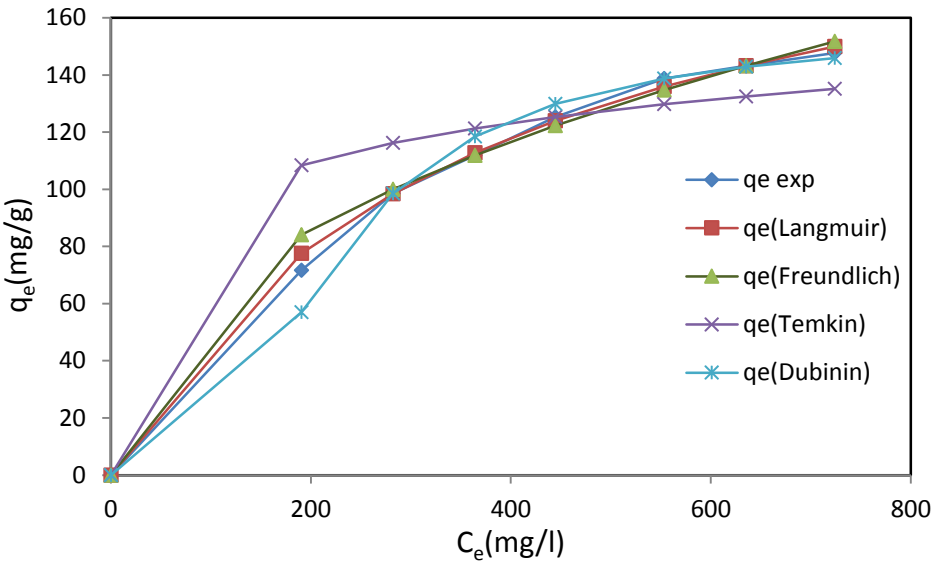

Figure 12: Comparison of data obtained experimentally for adsorption of Cd(II) ions onto pinewood sawdust treated with maleic acid (SWTMA) and two parameter isothermal models used to analyse the data.

Table 3 shows that the two-parameter isotherm models are ordered, in terms of best fit to the experimental data, as: Langmuir> Freundlich > Dubinin-Radushkevich> Temkin; while Table 4 shows that the three-parameter isotherm models were determined to be in the order: Sips > Khan> Toth > Redlich-Peterson, for the best fit to the data. As may be expected from the increase if fitting variables, the three-parameter models were consistently found to provide a better fit to the experimental data than two-parameter models. Overall, the eight isotherm models can be presented in the following order of fitness, based on the correlation coefficient (R^2) and error functions used in this study: Sips > Khan >Toth > Redlich-Peterson > Langmuir>Freundlich > Dubinin-Radushkevich> Temkin. The data were best fitted to Sips isotherm model. As this trend suggests, from all of the models used for analysis of the experimental data, the Sips isotherm model gave the highest R^2 value, as well as the lowest ARE, APE %, χ^2 and HYBRID error functions values, indicating that it gave the best overall fit to the data explaining the equilibrium adsorption of Cd (II) onto SDTMA (Figures 12 and 13).

This model is a combined of Langmuir and Freundlich expressions developed to predict the heterogeneous adsorption systems. Therefore at low adsorbate concentration, β = 0, this model

482 reduces to the Freundlich model, but at high concentration of adsorbate, β = 1, it predicts the
483 Langmuir model (monolayer adsorption).

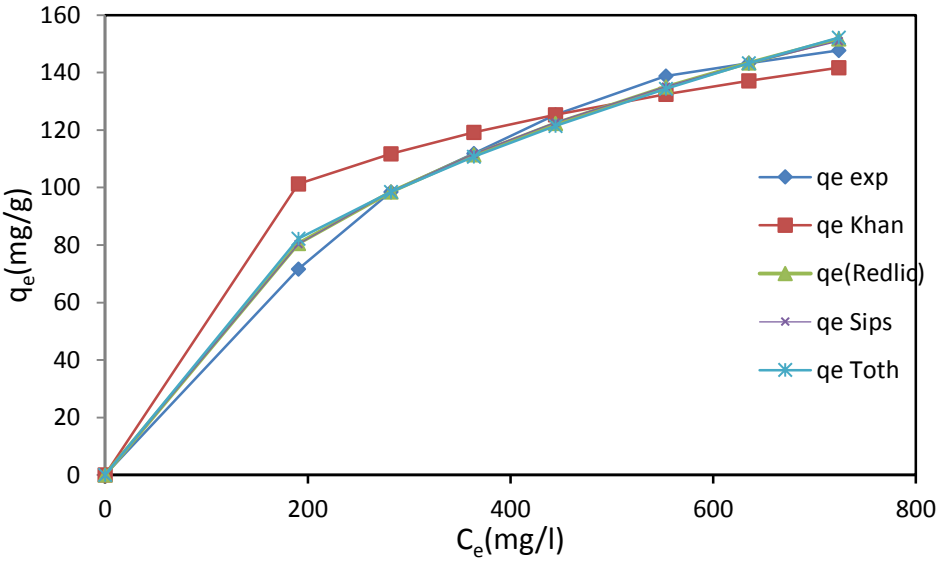

484
485

486 **Figure 13:** Comparison of data obtained experimentally for adsorption of Cd(II) ions onto pinewood sawdust
487 treated with maleic acid (SWTMA) and three-parameter isothermal models used to analyse the data

488

489 **Table 3:** Isotherm constants of two-parameter models for Cd(II) ions adsorption onto SDTMA at 303 K

Isotherm Model	Parameter	Value	Error Analysis	Value
Langmuir	a_L	0.002756	**ARE**	0.1369
	R_L	0.276	**APE%**	1.9554
	k_L	0.620304	**Hybrid**	0.6010
	Q_{max}	225.0379	R^2	0.9995
			χ^2	9.9526
Freundlich	n	2.256288	**ARE**	0.2691
	K_F	8.199321	**APE%**	3.8450
			Hybrid	2.4764
			R^2	0.9980
			χ^2	18.5262
Temkin	A_T	1.154914	**ARE**	1.0020
	b_T	125.4493	**APE%**	14.3143
			Hybrid	25.2684
			R^2	0.9787
			χ^2	73.1503
Dubinin-Radushkevich	q_D	156.5302	**ARE**	0.3156
	B_D	14.67483	**APE%**	4.5083
			Hybrid	3.5906
			R^2	0.9973
			χ^2	20.4253

490

491
492
493 **Table 4:** Isotherm constants of three-parameter models for Cd(II) ions adsorption onto SDTMA at 303 K

Isotherm Model	Parameter	Value	Error Analysis	Value
Redlich-Peterson	kg	1.379004	**ARE**	0.2093
	α_R	0.064915	**APE%**	2.9897
	g	0.676384	**Hybrid**	1.4088
			R^2	0.9988
			χ^2	15.4557
Toth	k_t	7.289696	**ARE**	0.2500
	a_t	0.08939	**APE%**	3.5716
	1/t	0.538547	**Hybrid**	1.9627
			R^2	0.9983
			χ^2	18.4182
Sips	K_s	2.567092	**ARE**	0.1944
	a_s	0.007467	**APE%**	2.7770
	B_s	0.706641	**Hybrid**	1.2952
			R^2	0.9989
			χ^2	13.9028
Khan	Q_{max}	191.43	**ARE**	0.74147
	a_k	1	**APE%**	10.5924
	b_k	0.004389	**Hybrid**	15.2881
			R^2	0.9879
			χ^2	51.1072

494

495

3.6. Adsorption kinetics

In addition to studying the equilibrium behaviour of adsorption systems, it is critical to understand their approach to this equilibrium by also studying the kinetics of adsorption, which can provide insight into the mechanism of adsorption. In this work, five models were used to model the kinetics of Cd(II)adsorption onto SDTMA: pseudo-first-order, pseudo second-order, Bangham, Elovich. The intraparticle diffusion model is not appropriate for studies at high adsorption times. To understand the adsorption mass transfer, the use of approximated models like Weber-Morris (intraparticle diffusion model), is not recommended. Weber-Morris is only valid for short adsorption times and when the bulk concentration is little affect. The Kinetic parameters calculated for this study and normalized standard deviation (Δq(%)) for adsorption of Cd (II) ions onto SDTMA at 303 K are summarised in Table 5.

Table 5: Kinetic parameters and normalized standard deviation (Δq(%)) for adsorption of Cd (II) ions onto SDTMA at 303 K

Models	Parameters	Values
		(300 mg/l)
Pseudo-first order	k_1	0.1073
	q_e	156.6542
	R^2	0.9866
	Δq(%)	14.8043
Pseudo-second order	K_2	0.0031
	q_e	157.9997
	R^2	0.9987
	Δq(%)	0.0150
Bangham's Equation	q_e	150.4382
	n	1.0910
	K_b	0.0933
	R^2	0.9838
	Δq(%)	15.5234
Elovich Equation	α	15
	β	0.03
	R^2	0.867502
	Δq(%)	26.81438169

511 The highest R^2 and lowest Δq% values were obtained for the pseudo second-order kinetic model, and
512 indicate that this provides the best fit model to the experimental data for the kinetics of Cd(II)
513 adsorption onto SDTMA (Figure 14), suggesting chemical control of the adsorption process. Overall,
514 the results obtained from the five kinetic models show that the adsorption kinetic models can be
515 ordered: pseudo second-order> Bangham> intra-particle > pseudo first-order > Elovich for the quality
516 of fit that they provide for the adsorption of Cd(II) ions onto SDTMA.

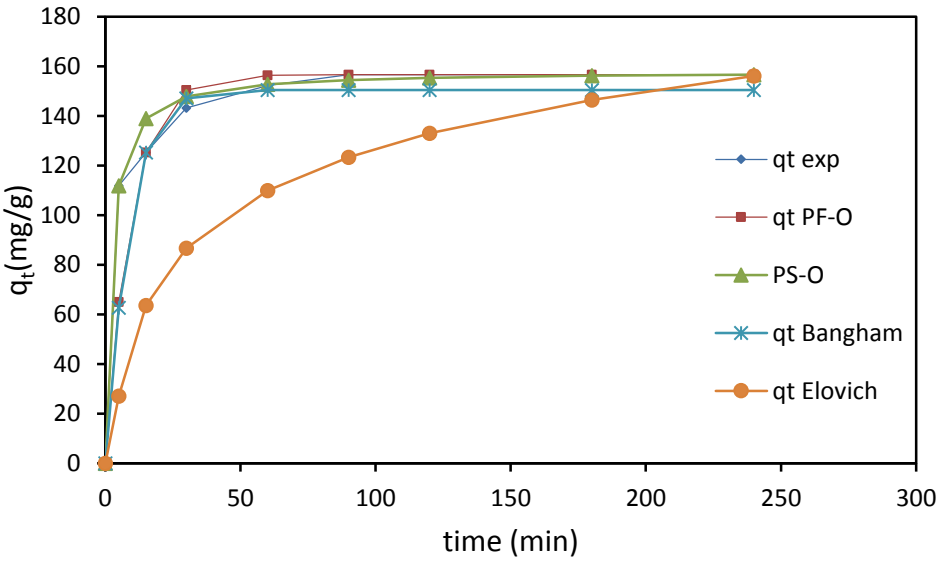

517

518 **Figure 14:** Comparison of data obtained experimentally for adsorption of Cd(II) ions onto pinewood sawdust
519 treated with maleic acid (SWTMA) and kinetic models used to analyse the data.

520

521 It can be concluded that the adsorption process obeyed the pseudo-second-order kinetic model and
522 the adsorption isotherm followed sips isotherm equation, demonstrating that the adsorption process
523 of Cd(II) onto SDTMA is heterogeneous adsorption systems and dominated by the chemical
524 adsorption.

525

526

527 **3.7. Mechanism of adsorption**

528 The process of metal ion remediation from aqueous systems by agricultural adsorbents is still not fully
529 understood due to the different interactions between the adsorbate and adsorbent, and the nature

of the adsorbent structure. In this study, cadmium hydroxide $Cd(OH)_2$ is the dominant form of the Cd(II) species in solution at pH > 7., while the dominant species at pH < 7 are $Cd(OH)^+$ and Cd^{2+}ions. The adsorption capacity is affected by the interaction of the adsorbent surface with these metal ion species. The highest adsorption capacity of SDTMA for Cd (II) ions was observed at pH 6, which is close to the pH based on zeta potential analysis. Thus, the interaction of dominant species (Cd^{2+} and $Cd(OH)^+$) at pH < 7, with the functional groups on the SDTMA surface, leads to an enhanced adsorption capacity at this optimum pH. The adsorption mechanism of porous adsorbents includes diffusion of ions to the external surface and into the pores of adsorbent, before ion exchange with the hydrogen ions associated with the carboxyl groups in SDTMA. The mechanism of CD(II) ion adsorption by SDTMA could also be due to complexation (Scheme 2), as well as physisorption and ion-exchange, and this may explain the results observed for adsorbent dosing, where increased accessibility of carboxyl groups from additional SDTMA may well increase the amount of complexation within the system.

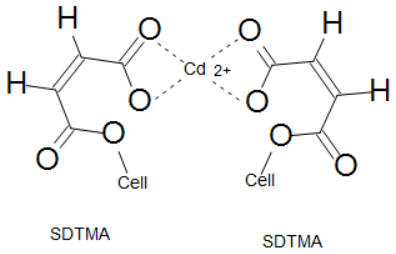

Scheme 2: The proposed complex structure formed between pinewood sawdust treated with maleic acid (SDTMA) and Cd(II) ions.

4. Conclusions

The adsorbent prepared within this study (SDTMA), formed via the treatment of pinewood sawdust (SD) with maleic acid, was used for the removal of Cd(II) ions from aqueous solutions. It was shown that the adsorption capacity of SDTMA was affected by adsorbent dose, pH, contact time and metal ion concentration in solution. SD and SDTMA samples were analysed for morphological and chemical characteristics, showing a clear modification of the treated sample. The data obtained for adsorption of Cd(II) ions on SDTMA was analysed using a suite of two-parameter (Langmuir, Freundlich and

553 Temkin, Dubinin-Radushkevich) and three-parameter (Redlich–Peterson, Toth, Sips, and Khan)
554 isotherm models, with goodness of fit determined using the nonlinear regression. Analysis showed
555 that the Sips model provided the best fit of the experimental data, while the maximum adsorption
556 capacity was 180.4 mg g^{-1}, at 303 K and adsorption was a favourable process. The kinetics of
557 adsorption of Cd(II) onto SDTMA were analysed using pseudo-first-order, pseudo-second-order,
558 Elovich and Bangham kinetic models, with the data described well by the pseudo second-order model,
559 suggesting overall chemical control of the adsorption process, which may be controlled by a
560 combination of physisorption, ion-exchange and complexation. Consequently, SDTMA has been
561 shown to be an effective adsorbent for the removal of Cd(II) ions from aqueous solutions, and
562 demonstrates the potential of agricultural wastes in water remediation processes.

References

[1] C.B. Godiya, X. Cheng, G. Deng, D. Li, X. Lu
Silk fibroin/polyethylenimine functional hydrogel for metal ion adsorption and upcycling utilization
Journal of Environmental Chemical Engineering, 7(2019) 102806

[2] V.F. Meseguer, J.F. Ortuño, M.I. Aguilar, M.L. Pinzón-Bedoya, M. Lloréns, J. Sáez, A.B. Pérez-Marín
Biosorption of cadmium (II) from aqueous solutions by natural and modified non-living leaves of Posidonia oceanica
Environmental Science and Pollution Research, 23 (2016) 24032-24046.

[3] X Xie, H Gao, X Luo, T Su, Y Zhang, Z Qin
Polyethyleneimine modified activated carbon for adsorption of Cd(II) in aqueous solution Journal of Environmental Chemical Engineering, 7 (2019) 103183

[4] A. Usman, A. Sallam, M. Zhang, M. Vithanage, M. Ahmad, A. Al-Farraj, Y.S. Ok, A. Abduljabbar, M. Al-Wabel
Sorption process of date palm biochar for aqueous Cd (II) removal: Efficiency and mechanisms
Water, Air, & Soil Pollution, 227 (2016) 449.

[5] P.B. Vilela, C.A. Matias, A. Dalalibera, V. A. Becegato, A.T. Paulino
Polyacrylic acid-based and chitosan-based hydrogels for adsorption of cadmium: Equilibrium isotherm, kinetic and thermodynamic studies.
Journal of Environmental Chemical Engineering 7 (2019) 103327

[6] A. Hashem, A. Al-Anwar, N.M. Nagy D.M. Hussein, S. Eisa
Isotherms and kinetic studies on adsorption of Hg (II) ions onto Ziziphus spina-christi L. from aqueous solutions
Green Processing and Synthesis, 5 (2016) 213-224.

[7] A. Hashem, H.A. Hammad, A. Al-Anwar
Modified Camelorum tree particles as a new adsorbent for adsorption of Hg (II) from aqueous solutions: kinetics, thermodynamics and non-linear isotherms
Desalination and Water Treatment, 57 (2016) 23827-23843.

[8] J.-S. Kwon, S.-T. Yun, J.-H. Lee, S.-O. Kim, H.Y. Jo
Removal of divalent heavy metals (Cd, Cu, Pb, and Zn) and arsenic (III) from aqueous solutions using scoria: kinetics and equilibria of sorption
Journal of Hazardous Materials, 174 (2010) 307-313.

[9] A. Khalil, H. Sokker, A. Al-Anwar, A.A. El-Zaher, A. Hashem

Preparation, Characterization and Utilization of Amidoximated Poly (AN/MAA)-grafted Alhagi Residues for the Removal of Zn (II) Ions from Aqueous Solution
Adsorption Science & Technology, 27 (2009) 363-382.

[10] X. Chen, R. Xu, Y. Xu, H. Hu, S. Pan, H. Pan
Natural adsorbent based on sawdust for removing impurities in waste lubricants
Journal of hazardous materials, 350 (2018) 38-45.

[11] S. Sirusbakht, L. Vafajoo, S. Soltani, S. Habibi
Sawdust Bio sorption of Chromium (VI) Ions from Aqueous Solutions
Chemical Engineering Transactions, 70 (2018) 1147-1152.

[12] A. Hashem, A. Azzeer, A. Ayoub
The Removal of Hg (II) Ions from Laboratory Wastewater onto Phosphorylated Haloxylon ammodendron: Kinetic and Equilibrium Studies
Polymer-Plastics Technology and Engineering, 49 (2010) 1463-1472.

[13] T.S. Anirudhan, M.K. Sreedhar
Adsorption thermodynamics of Co(II) on polysulphide treated sawdust
Indian J. Chem. Technol. 5 (1998) 41.

[14] C. Raji, T.S. Anirudhan
Copper-impregnated sawdust carbon for the treatment of as (III) rich
water J. Sci. Ind. Res. 57 (1998) 10.

[15] M. Ajmal, R.A. Rao, B.A. Siddiiqui
Studies on removal and recovery of Cr(VI) from electroplating wastes
Water Res. 30 (1996) 1478.

[16] S.R. Shukla, V.D. Sakhardande
Studies on metal ion removal by dyed cellulosic materials
Appl. Polym. Sci. 44 (1992) 903

[17] R. Suemitsu, M. Osako, N. Tagiri
Use of dye-treated sawdust for removal of heavy metals from wastewater
Sci. Eng. Rev. 27 (1986) 41

[18] K.S. Low, C.K. Lee, S.M. Make
Sorption of copper and lead by citric acid modified wood
Wood Science and Technology 38(2004) 629–640.

[19] M. Marchetti, A. Clement, B. Loubinoux, P. Gerardin

Decontamination of synthetic solutions containing heavy metals using chemically modified sawdusts bearing polyacrylic acid chains
Journal of Wood Science, 46(200) 331–333.

[20] R. Saliba, H. Gauthier, R. Gauthier
Adsorption of heavy metal ions on virgin and chemically-modified lignocellulosic materials
Adsorption Science and Technology 23 (2005) 313–322

[21] M. Gaey, V. Marchetti, A. Clement, B. Loubinoux, P. Gerardin
Decontamination of synthetic solutions containing heavy metals using chemically modified sawdusts bearing polyacrylic acid chains. Journal of Wood Science 46(2000) 331–333.

[22] G. Limousin, J.P. Gaudet, L. Charlet, S. Szenknect, V. Barthes, M. Krimissa
Sorption isotherms: a review on physical bases, modeling and measurement
Appl. Geochem. 22 (2007) 249–275

[23] S.J. Allen, G. Mckay, J.F. Porter
Adsorption isotherm models for basic dye adsorption by peat in single and binary component systems
J. Colloid Interface Sci. 280 (2004) 322–333

[24] M. Khalil, A. Hashem, A. Hebeish
Carboxymethylation of maize starch
Starch-Stärke, 42 (1990) 60-63

[25] I. Langmuir
The constitution and fundamental properties of solids and liquids. Part I. Solids
Journal of the American chemical society, 38 (1916) 2221-2295.

[26] K.R. Hall, L.C. Eagleton, A. Acrivos, T. Vermeulen
Pore-and solid-diffusion kinetics in fixed-bed adsorption under constant-pattern conditions
Industrial & Engineering Chemistry Fundamentals, 5 (1966) 212-223.

[27] H. Freundlich
Über die adsorption in lösungen
Zeitschrift für physikalische Chemie, 57 (1907) 385-470.

[28] M. Temkin
Kinetics of ammonia synthesis on promoted iron catalysts
Acta physiochim. URSS, 12 (1940) 327-356.

[29] M. Dubinin
The equation of the characteristic curve of activated charcoal

661 Dokl. Akad. Nauk. SSSR., 1947, pp. 327-329.
662 [30] O. Redlich, D.L. Peterson
663 **A useful adsorption isotherm**
664 Journal of Physical Chemistry, 63 (1959) 1024-1024.
665 [31] J. Toth
666 **State equation of the solid-gas interface layers**
667 Acta chim. hung., 69 (1971) 311-328.
668 [32] R. Sips
669 **On the structure of a catalyst surface**
670 The Journal of Chemical Physics, 16 (1948) 490-495
671 [33] A. Khan, R. Ataullah, A. Al-Haddad
672 **Equilibrium adsorption studies of some aromatic pollutants from dilute aqueous solutions on**
673 **activated carbon at different temperatures**
674 Journal of colloid and interface science, 194 (1997) 154-165.
675 [34] M. Hossain, H. Ngo, W. Guo
676 **Introductory of Microsoft Excel SOLVER function-spreadsheet method for isotherm and kinetics**
677 **modelling of metals biosorption in water and wastewater**
678 Journal of Water Sustainability, 3(2013) 223–237
679 [35] A. Kapoor, R. Yang
680 **Correlation of equilibrium adsorption data of condensible vapours on porous adsorbents**
681 Gas Separation & Purification, 3 (1989) 187-192.
682 [36] S. Karaca, A. Gürses, M. Ejder, M. Açıkyıldız
683 **Kinetic modeling of liquid-phase adsorption of phosphate on dolomite**
684 Journal of Colloid and Interface Science, 277 (2004) 257-263.
685 [37] J. Ng, W. Cheung, G. McKay
686 **Equilibrium studies of the sorption of Cu (II) ions onto chitosan**
687 Journal of Colloid and Interface Science, 255 (2002) 64-74
688 [38] S. Rangabhashiyam, N. Anu, M.G. Nandagopal, N. Selvaraju
689 **Relevance of isotherm models in biosorption of pollutants by agricultural byproducts**
690 Journal of Environmental Chemical Engineering, 2 (2014) 398-414.
691 [39] S.K. Lagergren
692 **About the theory of so-called adsorption of soluble substances**
693 Sven. Vetenskapsakad Handingarl, 24 (1898) 1-39

694 [40] P. Barkakati, A. Begum, M.L. Das, P.G. Rao
695 **Adsorptive separation of Ginsenoside from aqueous solution by polymeric resins: Equilibrium,**
696 **kinetic and thermodynamic studies**
697 Chemical Engineering Journal, 161 (2010) 34-45.
698 [41] C. Aharoni, M. Ungarish
699 Kinetics of activated chemisorption. Part 1.—The non-elovichian part of the isotherm
700 Journal of the Chemical Society, Faraday Transactions 1: Physical Chemistry in Condensed Phases,
701 72 (1976) 400-408.
702 [42] W. Gan, L. Gao, X. Zhan, J. Li
703 **Preparation of thiol-functionalized magnetic sawdust composites as an adsorbent to remove**
704 **heavy metal ions**
705 Rsc Advances, 6 (2016) 37600-37609
706 [43] M.L. Dianu, A. Kriza, N. Stanica, A.M. Musuc
707 **Transition metal M (II) complexes with isonicotinic acid 2-(9-anthrylmethylene)-hydrazide**
708 J. Serb. Chem. Soc, 75 (2010) 1515-1531.
709 [44] C. Teaca, R. Bodîrlau, I. Spiridon
710 **Maleic anhydride treatment of softwood –effect on wood structure and properties**
711 Cellulose Chem. Technol., 48 (2014) 863-868
712 [45] B. Hermawan, S. Nikmatin, Sudaryanto, H. Alatas, S.G. Sukaryo
713 **Effect of oil palm empty fruit bunches fibers reinforced polymer recycled**
714 Materials Science and Engineering 223 (2017) 012064
715 [46] B. Hermawan, S. Nikmatin, H. Alatas, Sudaryanto, S.G. Sukaryo
716 **Molecular analysis on the utilization of oil palm empty fruit bunches fiber as reinforcement for**
717 **acrylonitrile butadiene styrene biocomposites**
718 Earth and Environmental Science 65 (2017) 012028
719 [47] A. Hashem, A. Abdel-Lateff, S. Farag, D. Hussein
720 **Treatment of alhagi residues with tartaric acid for the removal of Zn (II) ions from aqueous**
721 **solution**
722 Adsorption Science & Technology, 26 (2008) 661-678
723 [48] O. Hamdaoui
724 **Batch study of liquid-phase adsorption of methylene blue using cedar sawdust and crushed brick**
725 Journal of hazardous materials, 135 (2006) 264-273.
726 [49] W.W. Ngah, L. Teong, R. Toh, M. Hanafiah

Utilization of chitosan–zeolite composite in the removal of Cu (II) from aqueous solution: adsorption, desorption and fixed bed column studies
Chemical Engineering Journal, 209 (2012) 46-53.

[50] M. Martín-Lara, F. Hernáinz, M. Calero, G. Blázquez, G. Tenorio
Surface chemistry evaluation of some solid wastes from olive-oil industry used for lead removal from aqueous solutions
Biochemical Engineering Journal, 44 (2009) 151-159

[51] H. Chen, Y. Zhao, A. Wang
Removal of Cu (II) from aqueous solution by adsorption onto acid-activated palygorskite
Journal of Hazardous Materials, 149 (2007) 346-354

[52] A. Hashem, H.A. Hussein, M.A. Sanousy, E. Adam, E.E. Saad
Monomethylolated thiourea–sawdust as a new adsorbent for removal of Hg (II) from contaminated water: equilibrium kinetic and thermodynamic studies
Polymer-Plastics Technology and Engineering, 50 (2011) 1220-1230

[53] S. Abdel-Aal, Y. Gad, A. Dessouki
The use of wood pulp and radiation-modified starch in wastewater treatment
Journal of applied polymer science, 99 (2006) 2460-2469

[54] S. Andini, R. Cioffi, F. Montagnaro, F. Pisciotta, L. Santoro
Simultaneous adsorption of chlorophenol and heavy metal ions on organophilic bentonite
Applied clay science, 31 (2006) 126-133.

[55] N. Azouaou, Z. Sadaoui, A. Djaafri, H. Mokaddem
Adsorption of cadmium from aqueous solution onto untreated coffee grounds: Equilibrium, kinetics and thermodynamics
Journal of hazardous materials, 184 (2010) 126-134

[56] N. Balkaya, H. Cesur
Adsorption of cadmium from aqueous solution by phosphogypsum
Chemical engineering journal, 140 (2008) 247-254.

[57] M.S. Berber-Mendoza, R. Leyva-Ramos, P. Alonso-Davila, J. Mendoza-Barron, P.E. Diaz-Flores
Effect of pH and temperature on the ion-exchange isotherm of Cd (II) and Pb (II) on clinoptilolite
Journal of Chemical Technology & Biotechnology: International Research in Process, Environmental & Clean Technology, 81 (2006) 966-973

[58] A. Borzou, M. Kalbasi, M. Hoodaji, M. Abdouss, A. Mohammadi

Isotherm investigation of the adsorption of cadmium onto modified poly (ethylene terephthalate) fiber

European Journal of Experimental Biology, 4 (2014) 136-142

[59] M. Geay, V. Marchetti, A. Clément, B. Loubinoux, P. Gérardin

Decontamination of synthetic solutions containing heavy metals using chemically modified sawdusts bearing polyacrylic acid chains

Journal of Wood Science, 46 (2000) 331-333.

[60] R. Say, A. Denizli, M.Y. Arıca

Biosorption of cadmium (II), lead (II) and copper (II) with the filamentous fungus Phanerochaete chrysosporium

Bioresource Technology, 76 (2001) 67-70.

[61] S.M. Dal Bosco, R.S. Jimenez, W.A. Carvalho

Removal of toxic metals from wastewater by Brazilian natural scolecite

Journal of Colloid and Interface Science, 281 (2005) 424-431.

[62] A. Albadarin, C. Mangwandi, G. Walker, S. Allen, M. Ahmad

Biosorption Characteristics of Sawdust for the Removal of Cd(ii) Ions: Mechanism and Thermodynamic Studies

Chemical Engineering Transactions, 24(2011) 1297-1302